Chromium doped zinc selenide optical fiber lasers

JUSTIN R. SPARKS,[1,2,*] STEPHEN C. ARO,[1] RONGRUI HE,[1] MELANIE L. GOETZ,[2] JAMES P. KRUG,[1] SEAN A. MCDANIEL,[3] PATRICK A. BERRY,[3] GARY COOK,[3] KENNETH L. SCHEPLER,[3] PIER J. SAZIO,[4] VENKATRAMAN GOPALAN,[5] AND JOHN V. BADDING[1,5,6,**]

[1]*Department of Chemistry and Materials Research Institute, Pennsylvania State University, University Park, PA 16802, USA*
[2]*Department of Chemistry, Muhlenberg College, Allentown, PA 18104, USA*
[3]*Air Force Research Laboratory, Wright Patterson Air Force Base, Dayton, OH 45433, USA*
[4]*Optoelectronics Research Centre, University of Southampton, Southampton, SO17 1BJ, UK*
[5]*Department of Materials Science and Engineering and Materials Research Institute, Pennsylvania State University, University Park, PA 16802, USA*
[6]*Department of Physics, Pennsylvania State University, University Park, PA 16802, USA*
[*]jsparks@muhlenberg.edu
[**]*This manuscript is dedicated to the memory of Prof. John V. Badding.*

Abstract: The optical fiber geometry is known for rugged, high power laser sources that are preferred for many applications, but is typically limited to the visible and near-infrared regions of the electromagnetic spectrum due to the transmission limits of silica ($< 2\,\mu m$). This wavelength range could be extended into the mid-infrared using transition metal doped, crystalline II-VI optical gain media, but these materials cannot be fabricated into optical fibers using conventional glass drawing methods. An in-situ high pressure chemical vapor deposition method for the fabrication of silica-cladded ZnSe fiber cores uniformly doped with Cr^{2+} is reported. Optical pumping experiments reveal that these doped fibers exhibit threshold behavior and thus function as mid-infrared optical fiber lasers. Finite element calculations show that undesirable thermal effects common in bulk II-VI crystals are mitigated in the fiber geometry.

1. Introduction

Silica optical fiber lasers have emerged as compact, rugged, stable, and very high power sources of both continuous wave and ultrafast near-infrared light ($< 2\,\mu m$) that are preferred for many applications [1]. These advantages could be extended into other wavelength domains (e.g. $> 2\,\mu m$) if fiber lasers could be fabricated out of a range of materials beyond silica and other glasses [2]. For example, semiconductor optical gain media such as Cr^{2+}-doped zinc selenide (Cr^{2+}:ZnSe) and related crystalline transition metal-doped chalcogenides are very attractive for efficient infrared lasers tunable in the technologically important $2\,\mu m$ to $5\,\mu m$ mid-infrared region of the spectrum [3,4].

Cr^{2+}:ZnSe lasers share many desirable characteristics with Ti-sapphire lasers, a preferred source for a very wide range of continuous wave (CW) and pulsed applications, but emit in the $2\,\mu m$ to $3\,\mu m$ mid-infrared region of the spectrum rather than in the red and near-infrared. In particular, Cr^{2+} does not exhibit any excited state spin allowed transitions and the matrix ZnSe has a low phonon frequency of $250\,cm^{-1}$, which allows for the highest quantum yield known for the $2\,\mu m$ to $3\,\mu m$ mid-infrared region, near continuous vibronic emission, and room temperature operation [5,6]. Cr^{2+}:ZnSe also exhibits an exceptionally broad gain, making it potentially very attractive for ultrafast applications [7]. In addition, several other useful transition metal

chalcogenide gain media are known based on the II-VI semiconductors [8]. Lasers operating in the 2 μm to 3 μm wavelength range of Cr^{2+}:ZnSe and the 3.7 μm to 5.1 μm wavelength range of the closely related Fe^{2+}:ZnSe materials are sought after for chemical detection, biomedicine, infrared countermeasures, and astronomical applications. [4,9] The key remaining technological challenge to realization of high power of continuous wave Cr^{2+}:ZnSe and related lasers is overcoming thermal lensing, which limits the output power from static gain media to about 14 W and arises because of the large thermo-optic coefficient of ZnSe ($\frac{dn}{dT} = 70 \times 10^{-6}K^{-1}$) [10–12]. Recently, Moskalev et al. have reported Cr^{2+}:ZnSe rotating disk lasers producing up to 140 W [13]. However, the rotating elements in the cavity of these lasers are susceptible to mechanical degradation and misalignment.

Cr^{2+}:ZnSe fiber lasers have been proposed to overcome these difficulties, [14] as this geometry is preferred for many applications and may ultimately scale to higher powers. Optical fibers are less susceptible to thermal lensing and their long, circular cross-section, small diameter and thus high surface-area-to-volume ratio cores can radiate heat efficiently and uniformly in direction over 360° [15]. As a result, fibers are noted for higher power handling capabilities in comparison with bulk materials and can be coupled much more easily to other fibers and fiber devices, thus enabling all-fiber optoelectronics. Additionally, the long pathlength of optical fibers may allow for lower Cr^{2+} concentrations and a further reduction in the thermal load compared to bulk crystals. However, incongruent vaporization has precluded drawing II-VI materials at high temperatures using standard techniques.

Our group previously reported centimeters-long silica cladded intrinsic ZnSe core optical fibers with an optical loss of $<1\,dB\,cm^{-1}$ for mid-infrared waveguiding applications using a high pressure chemical vapor depsition (HPCVD) method [16,17]. The HPCVD process can be used to fabricate many semiconductor fibers with lengths from centimeters to meters in parallel [18]. In this work, novel Cr^{2+} doping chemistries that are compatible with the HPCVD process and the fabrication of a Cr^{2+}:ZnSe optical fiber laser are reported.

2. Results and discussion

For HPCVD, the organometallic precursors dimethylselenide ($(CH_3)_2Se$) and dimethylzinc ($(CH_3)_2Zn$) are pressurized with hydrogen as a carrier gas/reactant to 70 MPa. This mixture is then configured to flow down a microcapillary template microns to tens of microns or more in diameter. Heating of the capillary to 500 °C results in the deposition of a film that fills the capillary nearly completely. $(CH_3)_2Se$ and $(CH_3)_2Zn$ were selected as precursors because they allow for "reactant encapsulation" [16,17] such that reaction only occurs in the heated capillary and therefore pre-reaction in the precursor mixture before entering the heated zone is precluded. Such ZnSe fibers, fabricated by HPCVD can guide CW and pulsed powers approaching those of silica fibers: $>6\,MW\,cm^{-2}$ for CW and $\approx 4.5GW\,cm^{-2}$ for pulsed (see Methods).

However, these ZnSe fibers must be uniformly doped along their length at Cr^{2+} concentrations of 10^{18}-10^{19} cm^{-3} for lasing applications. [19] Excessive Cr^{2+} ions result in fluorescence quenching while low concentrations may limit laser optical power. Much effort has been focused on developing chromium thermal diffusion methods to meet the critical challenge of uniformly doping bulk ZnSe gain media, [20,21] although many groups have also investigated molecular beam epitaxy, [22] co-sputtering, [23] and physical vapor transport [24,25]. None of these methods can be readily adapted to the fiber geometry; diffusion doping in particular is limited to distances on the order of 1 mm [20,26]. Instead, we have developed a single step chemical synthesis for Cr^{2+} doping that can work together with the $(CH_3)_2Se$ and $(CH_3)_2Zn$ ZnSe fiber HPCVD chemistry.

Common volatile chromium CVD precursors such as chromium carbonyl decompose at temperatures too low (250 °C) to be compatible with the approximately 500 °C HPCVD ZnSe deposition temperature. The metallocene bis(cyclopentadienyl)chromium (II) ($(Cp)_2Cr$), decomposes at

higher, more compatible temperatures. Furthermore, the $(Cp)_2Cr$ molecule can be modified by adding R groups to the cyclopentadiene rings $((RCp)_2Cr)$ and provide opportunities to tune vapor pressure and reactivity. The pyrolysis reaction is shown in Fig. 1, where R = H, Et, or iPr.

The R groups alter the stability of the resulting ring product formed during the breaking of the RCp-Cr bond, and thus tune the pyrolysis of the precursor. For example, the effect of functionalization in ferrocene (bis (cyclopentadienyl) iron (II)) compounds has been investigated, where the addition of two tert-butyl groups onto each cyclopentadiene ring of ferrocene increased its rate of pyrolysis by as much as 300 times [27]. We primarily investigated $(Cp)_2Cr$ and bis(ethyl-cyclopentadienyl) chromium (II) $((EtCp)_2Cr)$; an exploration of bis(isopropyl-cyclopentadienyl) chromium (II) $((iPrCp)_2Cr)$ demonstrated that it was largely incompatible with the deposition temperatures used to deposit ZnSe due to its relative instability.

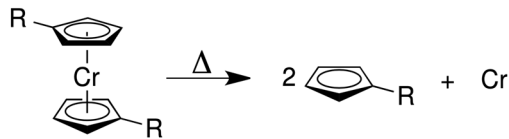**Fig. 1.** $(RCp)_2Cr$ pyrolysis, where R = H, Et, or iPr

The concentration of Cr^{2+} ions ultimately depends on both the stability of the precursor molecule at the deposition temperature used for ZnSe as well as the concentration of the precursor in the HPCVD stream, as determined by volatility. The evaporation rate of the liquid $(EtCp)_2Cr$ was determined to be approximatedly twice that of the solid $(Cp)_2Cr$ at 100 °C via a thermogravimetric analysis (see Supplement 1). Therefore, $(Cp)_2Cr$ is expected to be more stable than $(EtCp)_2Cr$, while $(EtCp)_2Cr$ is more volatile than $(Cp)_2Cr$ at a given temperature.

A key challenge in the codeposition of Cr^{2+} with ZnSe within silica capillaries is the need to introduce a low vapor pressure precursor into a high-pressure microfluidic reactant stream. An all-fiber microfluidic reaction vessel was fabricated using standard optical fiber fusion splicing techniques (Fig. 2(a) and S2). $(RCp)_2Cr$ is placed in a 150 μm diameter silica capillary fused to a smaller 15 μm capillary in which deposition occurs. $(CH_3)_2Se$ and $(CH_3)_2Zn$ with a hydrogen carrier gas/reactant at 70 MPa can be configured to flow into the microcapillary assembly. The heating of the two capillaries is adjusted independently to control both the vapor pressure of the chromium source in the larger capillary and the rate of deposition of Cr^{2+}:ZnSe in the smaller one (Fig. 2(a) and S2). Heating of the larger capillary to 200 °C with, for example, $(Cp)_2Cr$ in it vaporizes the precursor into the reactant stream such that deposition of Cr^{2+}:ZnSe can occur in the smaller capillary at 500 °C. The Cr^{2+}:ZnSe fills the capillary such that only a very small central pore remains, forming a fiber core.

Thus, the "microfluidic bubbler" HPCVD methodology allows solid, liquid, and gaseous precursors to all be used simultaneously. Low vapor pressure solids and liquids such as are required for Cr^{2+} doping of ZnSe, in particular, would be difficult to employ for HPCVD with traditional bubbler equipment without premature condensation. An additional advantage of the microfluidic doping approach is that much simpler and lower cost equipment (Figure S2) is employed in comparison with conventional chemical vapor deposition. The capillary fiber template itself becomes both the bubbler and the deposition chamber.

The deposited fiber core is of similar structural and optical quality to undoped ZnSe optical fibers (Fig. 2(b,c)) [16]. The central pore of the multimode step index optical optical fiber influences the guided mode (Fig. 2(d)) as previously reported, [17] with optical losses of $3.0\,dB\,cm^{-1}$ and $1.5\,dB\,cm^{-1}$ at 1.310 μm and 2.290 μm, respectively. Between these two wavelengths, the optical loss is expected to increase as a result of Cr^{2+} absorption. Comparison of the normalized infrared spectral absorbance of the Cr^{2+}:ZnSe fiber cores with a bulk, diffusion
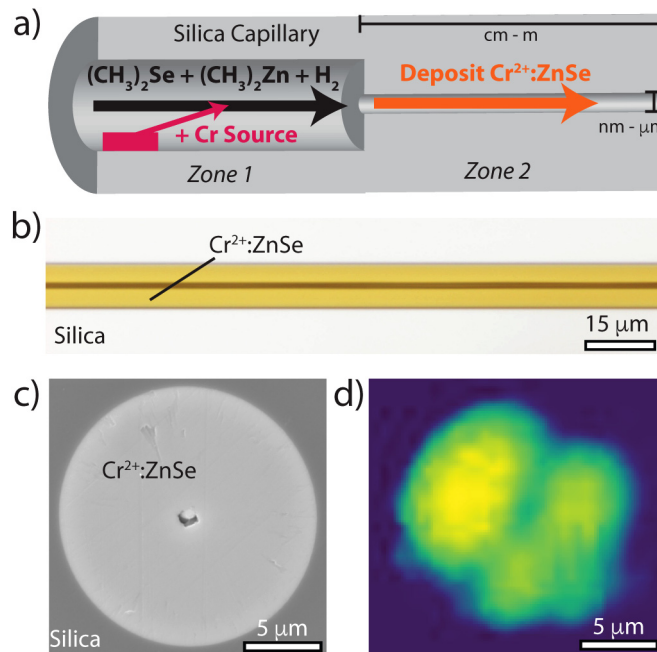
Fig. 2. Cr^{2+}:ZnSe optical fiber fabrication and characterization. a) Schematic of all-fiber apparatus with two independently heated furnace zones. Zone 1 heats a solid or liquid precursor contained in a larger capillary fusion spliced to the capillary in which the fiber core is deposited. The flowing reactant stream mixes with vapor from the heated Cr^{2+} precursor and continues to a higher temperature zone 2 where deposition of Cr^{2+}:ZnSe takes place. b) Diascopically illuminated optical micrograph along the length of a Cr^{2+}:ZnSe core optical fiber. The central pore is magnified considerably in comparison to its true diameter by a cylindrical lensing effect. c) Scanning electron micrograph of the Cr^{2+}:ZnSe fiber cross section. The central pore is approximately 450 nm in diameter. d) Image of the guided optical mode at 1.550 µm.

doped Cr^{2+}:ZnSe reference sample confirms the presence of chromium ions with the desired +2 oxidation state for laser gain media (Fig. 3). Normalized fluorescence spectra of both samples further confirm the presence of Cr^{2+} ions in the appropriate Zn^{2+} tetrahedral sites of the host lattice.

The effects of both vapor pressure and stability of the $(RCp)_2Cr$ precursor on the end concentration of Cr^{2+} in the material can be expected to be coupled. More volatile molecules will provide a higher concentration of chromium precursor in the HPCVD stream, while the less stable molecules will result in more precursor reaction and thus greater chromium incorporation. The impacts of precursor chemistry on the deposition reaction along the length of the fiber reaction chamber must also be considered. For example, too rapid or too slow a rate of precursor reaction could also lead to non-uniformity of the Cr^{2+} concentration along the length of the fiber.

Since the accurate direct measurement of the low concentrations of Cr^{2+} associated with doping is challenging, indirect spectroscopic methods such as infrared absorption or fluorescence are typically used instead [19]. The fluorescence spectra of the Cr^{2+}:ZnSe fiber cores were measured at different positions along the fiber length to qualitatively investigate the impact of precursor chemistry and reaction conditions on Cr^{2+} doping level and uniformity. The effects on chromium concentration as a function of source molecule at a fixed source temperature of 150 °C are shown in Table 1. A low source temperature of 150 °C with the solid, low vapor pressure

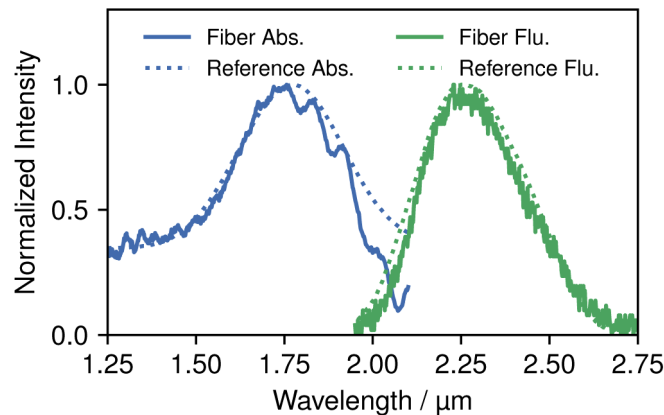**Fig. 3.** Spectroscopic characterization of Cr^{2+}:ZnSe fiber cores. Measured Cr^{2+}:ZnSe absorption and fluorescence (solid lines) from optical fibers deposited with $(EtCp)_2Cr$ and $(Cp)_2Cr$ as the source, respectively. Dotted lines are reference spectra from a commercial, diffusion doped Cr^{2+}:ZnSe bulk laser gain element.

$(Cp)_2Cr$ precursor, does not produce fiber cores with intense fluorescence, while those fabricated with the more volatile $(EtCp)_2Cr$ precursor display significant fluorescence. For comparison to diffusion based doping methods, an intrinsic ZnSe optical fiber was doped with Cr^{2+} using CrSe vapor diffusion at 900 °C for 24 h. The resulting fluorescence intensity of the material was similar to the HPCVD doping method, but limited to millimeter length scales from the fiber facet.

Table 1. Cr^{2+}:ZnSe fluorescence intensity for different cyclopentadiene ring substituents at a fixed source temperature of 150 °C. The precursor with the highest vapor pressure, $(EtCp)_2Cr$, deposits fiber cores with the highest fluorescence signal. The fluorescence intensity is similar to samples doped via diffusion.

Source	T / °C	Output Power / nW
CrSe Diffusion	-	1.05
$(Cp)_2Cr$	150	0.0005
$(EtCp)_2Cr$	150	1.39

Table 2 highlights the coupled nature of the process, with the liquid sources $((EtCp)_2Cr$ and $(iPrCp)_2Cr)$ at 150 °C and the solid $(Cp)_2Cr$ source at 225 °C, and also serves to illustrate the effects of chromium precursor stability on final chromium concentration uniformity. For each precursor, a fluorescence spectrum was measured at the two ends of a 1 cm long fiber sample. It can be seen that the doping level of $(EtCp)_2Cr$ and $(Cp)_2Cr$ is comparable at different source temperatures and is uniform over centimeter length scales, although more so for $(EtCp)_2Cr$, which indicates that their relative stabilities are compatible with the ZnSe deposition. Preliminary experiments with the $(iPrCp)_2Cr$ precursor showed a large difference in the emission intensity over a 1 cm fiber length. The portion of the deposited fiber closest to the HPCVD source has a much higher Cr^{2+} concentration than the downstream region, which indicates that the $(iPrCp)_2Cr$ precursor is not stable enough for the ZnSe chemistry and decomposes at too low of a temperature. However, the possibility that the $(iPrCp)_2Cr$ precursor produces very high doping levels, which would result in concentration quenching and a reduced fluorescence intensity, cannot be discounted. The $(EtCp)_2Cr$ precursor is therefore seen to be optimal for HPCVD as it allows for uniform doping, meaning it represents a good thermal match with ZnSe reaction chemistry

and produces Cr^{2+} concentrations similar to diffusion methods. Uniform dopant concentration is important for laser applications and represents a significant advance from diffusion doping methods. Additionally, this novel chemistry is not only useful for Cr^{2+}:ZnSe fiber cores, but should be readily adaptable to traditional CVD approaches for the fabrication of bulk crystals.

Table 2. Cr^{2+}:ZnSe fluorescence intensity for different ring substituents at source temperatures of 150 °C and 225 °C at two different positions along the length of the fiber core, separated by 1 cm (shown via ↔). The diffusion doped sample is shown for reference.

Source	T / °C	Output Power / nW		
CrSe Diffusion	-	1.05	↔	0.00
$(Cp)_2Cr$	225	2.24	↔	1.16
$(EtCp)_2Cr$	150	1.22	↔	1.39
$(iPrCp)_2Cr$	150	0.22	↔	0.03

To investigate the lasing properties of the Cr^{2+}:ZnSe optical fibers, a simple optical cavity was constructed by evaporating a gold high reflector on one facet of a polished, 0.5cm long sample. Fresnel reflection served as an output coupler on the opposite facet. This shorter segment of the ≈ 3cm long fabricated fiber was used to ensure uniform doping and central pore diameter. The fiber was pumped from the side with a 10 Hz, 10 ns pulse width pump laser with a wavelength of 1.700 μm (see Methods). A lasing threshold was observed in the total output power (collected with an InGaAs detector above 2 μm) versus input power plot (Fig. 4(a)). However, the emission energy was too weak to measure with conventional means, thus integrated counts were used. In the time domain, a sharp increase in output intensity with a lifetime (<500ns) much less than the Cr^{2+} fluorescence lifetime of 5 μs indicates that the cavity is above threshold and lasing in the gain switched regime (Fig. 4(b)), where the stimulated emission is reducing the lifetime.

A different laser geometry was used to investigate the lasing spectral emission (see Methods), where a sample was pumped using a custom-built Ho:YAG pulsed laser operating at 2.09 μm and delivering 10 kHz, 200 ns pulses. Above the lasing threshold, the output of the fiber laser is broad band and within the free-running gain bandwidth of Cr^{2+}:ZnSe, centered around 2.3 μm (Fig. 4(c)). The lasing wavelength is shorter than previous reports demonstrating channel waveguide lasers operating at 2.486 μm [28] and 2.6 μm [29]. It is likely that onset of absorption from the silica cladding above 2 μm is leading to this relatively short output wavelength, but it could also be indicative of lower chromium concentrations [30]. Additionally, the broad line-width is common in a free-running gain medium.

With further optimization of Cr^{2+}:ZnSe optical fiber fabrication, narrow line-width emission and CW operation may be realized. Finite element analysis has been used to estimate the upper limit of CW output power from a 15 μm Cr^{2+}:ZnSe core clad in silica. Although lasing operation is expected to reduce the heat load, at a certain point of pumping, a small increase in temperature will lead to an increased rate of non-radiative relaxation which in turn leads to decreased lasing and greater temperature rise. This feedback can continue until lasing stops completely [31]. Therefore, the upper limit of power is a result of balancing thermal effects and material damage thresholds. Using estimates of device performance based on published data to find the critical temperature (see Supplement 1 for full calculation details), a best case scenario for the Cr^{2+}:ZnSe optical fiber would have a slope efficiency of 0.83 (quantum limit) and a threshold pump power of 0.01 W. From this, a critical incident pump power of approximately 5.1 W can be calculated to result in 4.3 W of laser output from the fiber.

Due to its onset of absorption above 2 μm and low thermal conductivity, silica is not an ideal cladding material for Cr^{2+}:ZnSe. The effects of the silica cladding can be minimized by first depositing a ZnS or ZnS_xSe_{1-x} cladding before the Cr^{2+}:ZnSe core using previously reported HPCVD chemistries [17]. An even more effective approach would be to use diamond as a
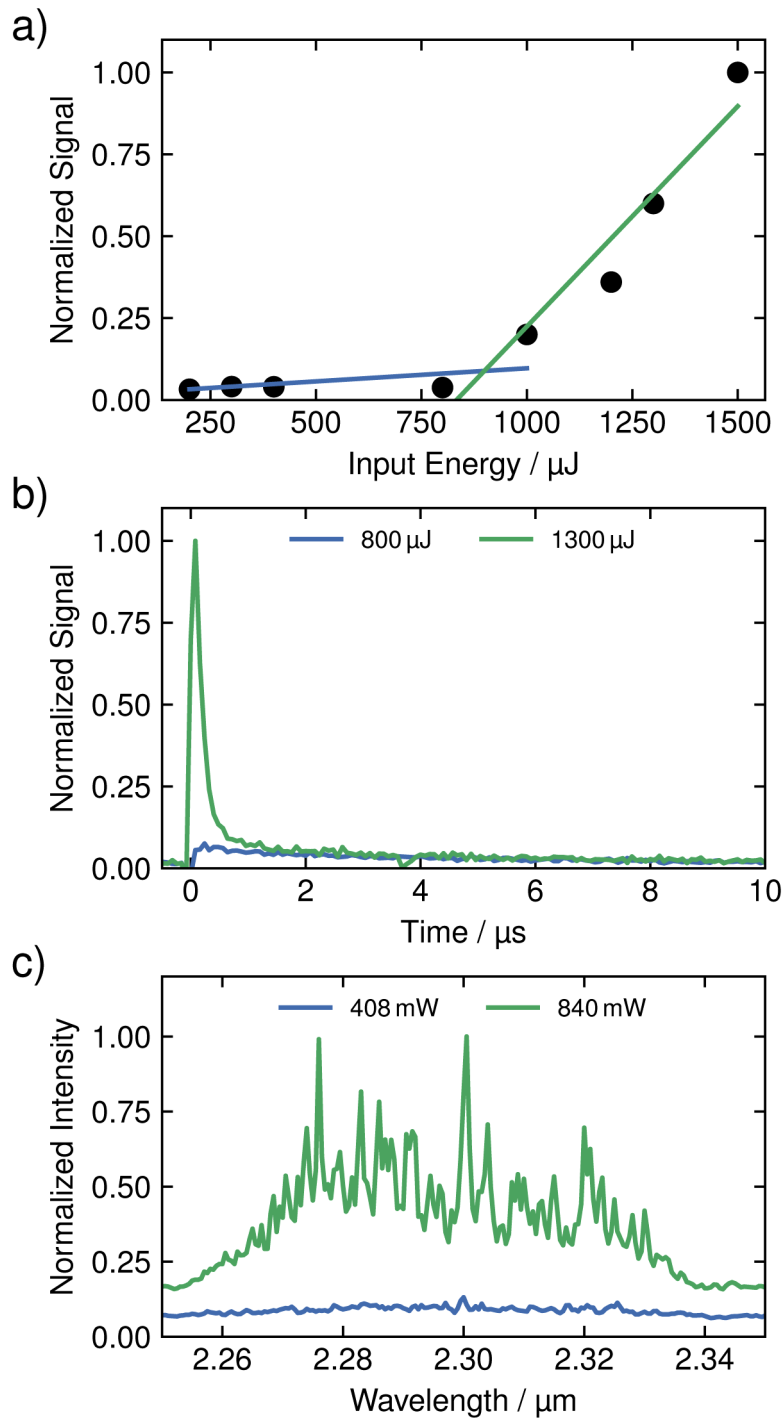
Fig. 4. Time domain and spectral emission characterization of the Cr^{2+}:ZnSe optical fiber. a) Optical pumping of a 15 µm Cr^{2+}:ZnSe optical fiber, where clear evidence of threshold behavior is observed. b) Sharpening of the output signal is seen in the time domain, indicating stimulated emission is accelerating the decay of the excited state. c) Spectral emission of Cr^{2+}:ZnSe fiber laser above and below the laser threshold.

cladding material [32]. In addition to controlling the mode structure, allowing lower order mode operation, such structures would have great potential to overcome thermal limitations. For example, with a diamond cladding, the laser output from a 15 μm Cr^{2+}:ZnSe core is estimated to reach 331 W, which is much greater than bulk laser elements and would be limited by the damage threshold of the material. The estimate of output power can be increased with larger core, multimode fibers, which are comparable to near-infrared silica fiber lasers that emit in the kW power regime.

3. Conclusions

We have demonstrated the first Cr^{2+}:ZnSe crystalline semiconductor optical fiber laser, operating in the gain-switched regime around 2.3 μm. The element was fabricated using a novel HPCVD reaction utilizing organometallic chromium precursors, which allows for control of the dopant incorporation during material growth. This new chemical approach offers the possibility of uniform doping levels despite the ultra-high aspect ratio of the fiber optics. The flexibility of the HPCVD technique allows for interesting future directions such as fabrication of Cr^{2+}:ZnSe-ZnS_xSe_{1-x} core-cladding structures for single mode operation, larger core structures to decrease waveguide losses and increase power-handling capability, as well as ternary host materials and iron doped gain media, allowing for operation of these devices across the mid-infrared.

4. Methods

4.1. Microscopy and spectroscopy

Samples for scanning electron microscopy (FEI Quanta 200) were prepared by mechanical polishing followed by coating in iridium. Waveguide measurements were performed with 1.310 μm and 1.550 μm diode lasers (Thorlabs) as well as a bulk Cr^{2+}:ZnSe laser (IPG Photonics). FTIR experiments were carried out using a Bruker Hyperion 3000 FTIR microscope. Light was coupled into a 50 μm core Cr^{2+}:ZnSe fiber using reflective optics and collected in the same way. Fluorescence measurements were carried out by pumping the samples with a 1.9 μm thulium fiber laser (IPG Photonics) at 500 mW. Light was coupled into each facet of 1 cm samples via an end-pump geometry using high NA, AR coated lenses and collected in the same way. The collected light was then directed to a 156 mm monochromator (Jarrell Ash Monospec 18) with a 300 g/mm grating and an extended range InGaAs single channel detector (Hamamatsu). Note that the fluorescence emission typically extends to 3 μm, but was limited to the detector sensitivity range.

4.2. Power handling characterization

CW power handling measurements were performed with a 1.9 μm thulium fiber laser (IPG Photonics) operating at 10 W, which was focused into a 15 μm diameter ZnSe fiber using an appropriate AR coated lens to match the core size of the fiber. Under these conditions, no damage to the optical fiber facet was observed. Pulsed damage threshold measurements were performed with a Mai Tai HP mode-locked Ti:sapphire femtosecond laser source operating at 0.950 μm with a 80 MHz repetition rate, a pulse duration of 100 fs, and 300 mW of average power. The light was focused using an AR coated lens to match the core size of an 11 μm ZnSe fiber. Damage to the optical fiber facet was observed at $\approx 4.5 \text{GW cm}^{-2}$.

4.3. Characterization of laser performance

For time domain measurements, a 10 Hz repetition rate, 10 ns pulse duration optical parametric oscillator (Spectraphysics) operating at 1.7 μm was used to pump the optical fiber laser in a side-pumped geometry. The pump beam was focused onto the core along a 5 mm long sample using a cylindrical lens (50 mm focal length). The cavity was formed with an evaporated gold

mirror on one facet ($\approx$ 100nm) and Fresnel reflection ($\approx$ 17%) as an output coupler from the other facet. The signal was collected from the output facet and passed through two 2 μm long-pass filters before being focused onto an extended range InGaAs single channel detector (Hamamatsu) and processed with a gated integrator and boxcar averager (Stanford Research Systems).

For spectral measurements, a sample was pumped using a home-built Ho:YAG pulsed laser operating at 2.09 μm and delivering 10 kHz, 200 ns pulses. No coating or other preparation was undertaken to minimize reflections at the core-air interface. The sample was inserted into a cavity consisting of a dichroic input coupler (transmission >97% at 1.9 μm to 2.1 μm, reflectivity >98% at 2.3 μm to 2.7 μm), through which it was pumped, and a partially reflective (90%) dielectric output coupler. A ZnSe lens, AR coated at the pump wavelength, was used to couple light into the sample, while a mid-infrared AR coated calcium fluoride lens was used to collect sample light, where it was directed to a 750 mm monochromator (Acton Research Corporation) equipped with an extended range InGaAs detector (Hamamatsu). Gain-switched lasing was seen to arise above 500 mW of average pump power, or 50 μJ per pulse, and the spectral output was stable and repeatable.

Funding

Disclosures

The authors declare no conflicts of interest.

Supplementary Materials

See Supplement 1 for supporting content.

References

1. J. Nilsson and D. N. Payne, "High-power fiber lasers," Science **332**(6032), 921–922 (2011).
2. S. D. Jackson, "Towards high-power mid-infrared emission from a fibre laser," Nat. Photonics **6**(7), 423–431 (2012).
3. R. H. Page, K. I. Schaffers, L. D. DeLoach, G. D. Wilke, F. D. Patel, J. B. Tassano, S. A. Payne, W. F. Krupke, K. Chen, and A. Burger, "Cr^{2+}-doped zinc chalcogenides as efficient, widely tunable mid-infrared lasers," IEEE J. Quantum Electron. **33**(4), 609–619 (1997).
4. S. Mirov, V. Fedorov, I. Moskalev, D. Martyshkin, and C. Kim, "Progress in Cr^{2+} and Fe^{2+} doped mid-IR laser materials," Laser Photonics Rev. **4**(1), 21–41 (2010).
5. S. Kück, "Spectroscopy and laser characteristics of Cr^{2+}-doped chalcogenide crystals - overview and recent results," J. Alloys Compd. **341**(1-2), 28–33 (2002).
6. S. Kueck, "Cr^{2+} lasers," in *International Conference on Lasers, Applications, and Technologies 2002: Advanced Lasers and Systems*, vol. 5137 G. Huber, I. A. Scherbakov, and V. Y. Panchenko, eds., International Society for Optics and Photonics (SPIE, 2003), pp. 48–59.
7. E. Sorokin, S. Naumov, and I. T. Sorokina, "Ultrabroadband infrared solid-state lasers," IEEE J. Sel. Top. Quantum Electron. **11**(3), 690–712 (2005).
8. L. D. DeLoach, R. H. Page, G. D. Wilke, S. A. Payne, and W. F. Krupke, "Transition metal-doped zinc chalcogenides: Spectroscopy and laser demonstration of a new class of gain media," IEEE J. Quantum Electron. **32**(6), 885–895 (1996).
9. T. J. Carrig, "Transition-metal-doped chalcogenide lasers," J. Electron. Mater. **31**(7), 759–769 (2002).
10. I. T. Sorokina, "Cr^{2+}-doped II-VI materials for lasers and nonlinear optics," Opt. Mater. **26**(4), 395–412 (2004).
11. P. A. Berry and K. L. Schepler, "High-power, widely-tunable Cr^{2+}:ZnSe master oscillator power amplifier systems," Opt. Express **18**(14), 15062–15072 (2010).
12. K. L. Schepler, R. D. Peterson, P. A. Berry, and J. B. McKay, "Thermal effects in Cr^{2+}:ZnSe thin disk lasers," IEEE J. Sel. Top. Quantum Electron. **11**(3), 713–720 (2005).
13. I. Moskalev, S. Mirov, M. Mirov, S. Vasilyev, V. Smolski, A. Zakrevskiy, and V. Gapontsev, "140 W Cr:ZnSe laser system," Opt. Express **24**(18), 21090–21104 (2016).
14. D. V. Martyshkin, J. T. Goldstein, V. V. Fedorov, and S. B. Mirov, "Crystalline Cr^{2+}:ZnSe/chalcogenide glass composites as active mid-IR materials," Opt. Lett. **36**(9), 1530–1532 (2011).
15. D. J. Richardson, J. Nilsson, and W. A. Clarkson, "High power fiber lasers: Current status and future perspectives," J. Opt. Soc. Am. B **27**(11), B63–B92 (2010).

16. J. R. Sparks, R. He, N. Healy, M. Krishnamurthi, A. C. Peacock, P. J. A. Sazio, V. Gopalan, and J. V. Badding, "Zinc selenide optical fibers," Adv. Mater. **23**(14), 1647–1651 (2011).

17. J. R. Sparks, R. He, N. Healy, S. Chaudhuri, T. C. Fitzgibbons, A. C. Peacock, P. J. A. Sazio, and J. V. Badding, "Conformal coating by high pressure chemical deposition for patterned microwires of II-VI semiconductors," Adv. Funct. Mater. **23**, 1647–1654 (2012).

18. J. R. Sparks, P. J. Sazio, V. Gopalan, and J. V. Badding, "Templated chemically deposited semiconductor optical fiber materials," Annu. Rev. Mater. Res. **43**(1), 527–557 (2013).

19. A. Sennaroglu, U. Demirbas, A. Kurt, and M. Somer, "Direct experimental determination of the optimum chromium concentration in continuous-wave Cr^{2+}:ZnSe lasers," IEEE J. Sel. Top. Quantum Electron. **13**(3), 823–830 (2007).

20. Y. F. Vaksman, V. V. Pavlov, Y. A. Nitsuk, Y. N. Purtov, A. S. Nasibov, and P. V. Shapkin, "Optical absorption and chromium diffusion in ZnSe single crystals," Semiconductors **39**(4), 377–380 (2005).

21. J. Ndap, K. Chattopadhyay, O. Adetunji, D. Zelmon, and A. Burger, "Thermal diffusion of Cr^{2+} in bulk ZnSe," J. Cryst. Growth **240**(1-2), 176–184 (2002).

22. M. Jouanne, J. Morhange, E. Dynowska, E. łLusakowska, W. Szuszkiewicz, L. Molenkamp, and G. Karczewski, "Structure characterization of MBE-grown (Zn,Cr)Se layers," J. Alloys Compd. **382**(1-2), 92–99 (2004).

23. N. Vivet, M. Morales, M. Levalois, X. Portier, and J. Doualan, "Structural and photoluminescence properties of Cr^{2+}:ZnSe films deposited by radiofrequency magnetron co-sputtering for mid-infrared microlaser applications," Mater. Sci. Eng., B **146**(1-3), 236–240 (2008).

24. C.-H. Su, S. Feth, M. Volz, R. Matyi, M. George, K. Chattopadhyay, A. Burger, and S. Lehoczky, "Vapor growth and characterization of Cr-doped ZnSe crystals," J. Cryst. Growth **207**(1-2), 35–42 (1999).

25. V. A. Akimov, M. P. Frolov, Y. V. Korostelin, V. I. Kozlovsky, A. I. Landman, Y. P. Podmar'kov, and A. A. Voronov, "Vapour growth of II-VI single crystals doped by transition metals for mid-infrared lasers," Phys. Status Solidi C **3**(4), 1213–1216 (2006).

26. U. Demirbas, A. Sennaroglu, and M. Somer, "Synthesis and characterization of diffusion-doped Cr^{2+}:ZnSe and Fe^{2+}:ZnSe," Opt. Mater. **28**(3), 231–240 (2006).

27. L. M. Dyagileva, E. I. Tsyganova, and Y. A. Aleksandrov, "The kinetic stability of biscyclopentadienyl and diarene compounds of transition metals in the thermal decomposition reaction," Russ. Chem. Rev. **57**(4), 316–325 (1988).

28. J. R. Macdonald, S. J. Beecher, P. A. Berry, G. Brown, K. L. Schepler, and A. K. Kar, "Efficient mid-infrared Cr:ZnSe channel waveguide laser operating at 2486nm," Opt. Lett. **38**(13), 2194–2196 (2013).

29. J. E. Williams, V. V. Fedorov, D. V. Martyshkin, I. S. Moskalev, R. P. Camata, and S. B. Mirov, "Mid-IR laser oscillation in Cr^{2+}:ZnSe planar waveguide," Opt. Express **18**(25), 25999–26006 (2010).

30. A. Sennaroglu, U. Demirbas, A. Kurt, and M. Somer, "Concentration dependence of fluorescence and lasing efficiency in Cr^{2+}:ZnSe lasers," Opt. Mater. **29**(6), 703–708 (2007).

31. P. A. Berry, J. R. Macdonald, S. J. Beecher, S. A. McDaniel, K. L. Schepler, and A. K. Kar, "Fabrication and power scaling of a 1.7 W Cr:ZnSe waveguide laser," Opt. Mater. Express **3**(9), 1250–1258 (2013).

32. I. Aharonovich, A. D. Greentree, and S. Prawer, "Diamond photonics," Nat. Photonics **5**(7), 397–405 (2011).